International Journal on Interactive Design and Manufacturing (IJIDeM)
https://doi.org/10.1007/s12008-023-01228-5

TECHNICAL PAPER

Experimental analysis of Inconel 625 alloy to enhance the dimensional accuracy with vibration assisted micro-EDM

Ashok Kumar Sharma[1] · Vishal Singh[1] · Ashish Goyal[1] · Ankit D. Oza[2] · Kiran S. Bhole[3] · Manoj Kumar[4]

Received: 19 November 2022 / Accepted: 30 January 2023

Abstract
With the continuous improvement in manufacturing processes there is an amalgamation of digital technology with traditional concepts. Electric discharge machining is one such example of it. The more industries digitalize it the more is the degree of automation. In present experimental work ZNC Electrical Discharge Machine has been used to perform the experiments. Total 18 experiments have been performed on Inconel 625 alloy as per the orthogonal array prepared by Minitab software. Tool electrode, peak current, pulse on time (T_{on}) and pulse of time (T_{off}) are considered as input parameters. There were two levels of tool and rest were assigned three levels. 9 experiments were conducted via copper tool without vibration and in remaining 9 experiments vibration assisted copper tool was used. Vibration was given to tool with coin vibration motor which was powered by battery. It was observed that when Toff was increased from 25 to 35 μs the surface roughness enhances by 23.23%. Also, it was found that circularity improves by 25.85% when Ton is raised from 140 to 160 μs. Surface roughness of each drilled hole was measured using surface roughness tester and circularity was measured using Quick Image. The FESEM and EDS has performed on the machined specimen to analyze the microstructure and chemical composition.

Keywords Surface roughness · Circularity · Inconel 625 alloy · Micro-EDM · Minitab

1 Introduction

The application of Inconel 625 is mainly in marine and petroleum industries. It is also known as Nicrofer 6020. No corrosion is observed if it deploys in steam line piping [1]. It is used below 1200°F the annealing treatment is mandatory. With this treatment its tensile strength can go up to 880 MPa. It has the ability to preserve toughness and ductility at lower temperature. Machining of such alloy are difficult by traditional methods [2]. Machining is done with the occurrence of multiple sparks. Dielectric liquid is present within tool and job system that is in spark gap. With the machine control button if it is semi-automatic tool is moved vertically downwards. As the optimum distance is achieved the buzzer creates sound. The parameters are edited based on the requirement. Save, load, and enter buttons are pressed. Then there is occurrence of spark and machining is carried depending upon the machining time given to the machine.

Mausam et al. [3] carry out the investigation on carbon fiber-based composite. When the pulse on time was raised from 120 to 180 microseconds with current being constant it was observed that material removal rate improves by 38%. And tool wear rate increases by 3.5%. When the peak current was increased from 1 to 5A in addition T_{on} increasing from 120 to 180 microseconds the material elimination rate becomes two-fold. Singh et al. [4] enhanced the performance of EDM by using low frequency vibration setup. When vibration was increased from 25 to 75 Hz in addition with

✉ Ashish Goyal
ashish.goyal@jaipur.manipal.edu

Ankit D. Oza
ankit.oza@iar.ac.in

Kiran S. Bhole
kiranbhole1977@gmail.com

Manoj Kumar
manojkumar@abes.ac.in

1 Department of Mechanical Engineering, Manipal University Jaipur, Jaipur 303007, India

2 Department of Computer Sciences and Engineering, Institute of Advanced Research, Gandhinagar, Gujarat 382426, India

3 Department of Mechanical Engineering, Sardar Patel College of Engineering, Munshi Nagar, Andheri West, Mumbai 400058, India

4 Department of Mechanical Engineering, ABES Engineering College, Ghaziabad, U.P. 201009, India

Published online: 05 March 2023

peak current from 10 to 15 A the material removal rate was increased by 10.7%. When current escalates from 5 to 20 A the surface roughness expands by 22% and tool wear rate becomes 4 times.

Teimouri et al. [5] investigated dry EDM process with the help of back propagation neural network. ANN optimization was used to predict the output performance with changes in input parameter. By comparative analysis of predictive model and experimental results it was concluded that artificial bee algorithm can determine optimum points accurately. Goyal et al. [6, 7] had conducted experiments with cryogenic treated wire on aerospace material to test the machinability and surface roughness. It was concluded that MRR expands with increase in T_{on}. When pulse on time was increased from 10 to 12 μs surface roughness decreased from 2.78 to 1.93 μm. Rajendra et al. [8] carried out investigation to analysis the accuracy and quality of micro holes in vibration assisted micro EDM. It was found that material elimination rate was more sensitive to voltage and capacitance. MRR enhances with increment in capacitance. Also, MRR first enhances with boost in voltage and after attaining optimum threshold it deteriorates again.

Teimouri et al. [9] modified the EDM machine with further attaching rotary system and gas supply setup was also incorporated. In rotary system the components were pulley belt mechanism, electro motor, and inverter to produce various levels of rotary velocities. It was concluded that brass tool's material elimination rate was higher than Cu may be due to lower electrical resistivity. Somashekhar et al. [10] performed the research on the micromachining center utilizing RC circuit. Objective was to optimize material elimination rate utilizing ANN and genetic algorithm. Voltage, feed rate, speed, and capacitance were used as the control factors. Feed forward neural network was used along the way utilizing back propagation algorithm. Neural network 4–6–6–1 very accurately predicted the material elimination rate. It was so accurate that avg prediction error for training was 0.8% and for testing it was 3.9%.

Srivastava et al. [11] made use of cryogenically cooled electrode which was ultrasonic vibration assisted with kerosene oil as dielectric fluid. It was concluded that electrode wear ratio and SR was significantly smaller in vibration assisted EDM as compared to traditional EDM. While the rate at which material elimination takes place was superior in traditional EDM.

Zhang et al. [12] investigated micro EDM with multi objective genetic algorithm and support vector machine to optimize processing time and electrode wear ratio. Orthogonal test results were utilized as training and testing data for SVM. It was observed that model was accurate. GA was utilized based on non-dominated sorting. Unune et al. [13] carried out their work on micro WEDM which was assisted with low frequency vibration on nickel based super alloy. It was evaluated that with vibration MRR improved very much significantly. The effect of vibration was very less on kerf widths. Kumar et al. [14] estimated the surface crack density and recast layer width in wire EDM. It was noticed that as T_{on} increases the surface crack density rises superiorly. When the value of peak current was increase from 120 to 200 A important impact on surface crack density was seen that is increment by 40%. Huu et al. [15] performed multi objective optimization on SKD61 steel machining with copper as tool electrode. Authors developed vibration setup to provide 128 to 512 Hz frequency. The quality indicators were surface roughness, material elimination rate and tool erosion rate. Taguchi in combination with TOPSIS, GRA and MOORA optimization was established on ratio examination. When peak current was increased from 3 to 8 A material elimination rate enhanced from 3 to 7 mm^3/min. Mohanty et al. [16] investigated EDM with intelligent approach called quantum behave particle swamp optimization. Their quality indicators were radial overcut, material elimination rate and tool erosion rate. When discharge current is increased from 3 to 7 A the MRR boosts from 11 to 22 mm^3/min. With increment in discharge voltage and T_{on}, the MRR decreases. Endo et al. [17] carried out experimental work on vibration assisted micro EDM. Analysis was performed to measure the impact of vibration on machining time and discharge stability. It was declared that there is substantial decline in machining time with vibration. Also, it was concluded that parallel vibration takes longer machining time as compared to perpendicular vibration. Rahul et al. [18] optimize the EDM parameter during machining of Inconel 718. Principal component analysis and quality loss concept was used for optimization. Author's optimum parameters were 11 A as peak current and 100 μs as pulse on time for highest material elimination rate, minimum surface roughness and least electrode tool wear.

Lee et al. [19] conducted experiments to analyze the effect of low frequency vibrations on micro EDM drilling setup. It was observed that metal cutting time was decreased by 60% at 60 Hz as compared to machining without vibration. Whereas in reverse EDM it was reduced by 25% at same input parameters. As the vibration amplitude raised from 2 to 8 μm the machining time was decreased. Kumar et al. [20] evaluated the surface roughness, material elimination rate and kerf width utilizing the genetic algorithm and grey entropy fuzzy optimization in wire EDM in DC53 steel grade. Pulse on time contributed the 53% for surface roughness and peak current involvement was 17%. In the case of material elimination rate the pulse on time involvement was 69% and of pulse of time was 23%. Le et al. [21] carried out their research in EDM and powder mixed EDM with and without application of vibration. With vibration assisted setup in EDM the rise in MRR was 35% at 600 Hz as compared to no vibration and in case of vibration assisted setup in powder mixed EDM the maximum increment in material elimination

rate was 96% at 400 Hz compared to no vibration. Kumaran et al. [22] carried out grey fuzzy optimization on carbon fiber reinforced plastic composite with epoxy in ultrasonic vibration assisted EDM. At 200 μs and 100 V the tool wear rate was observed minimum, and it was $0.4*10^{-4}$ g/min. The involvement of capacitance in deburring was 63% of pulse of time was 29%. Nguyen et al. [23] experimented on low frequency aided EDM to optimize MRR and surface roughness. TOPSIS with Taguchi was incorporated for multi objective optimization. It was found out that with low frequency it was possible to improve the material elimination because one can control the spark energy. The optimal parameters evaluated using TOPSIS optimization were 86% accurate. Pandey et al. [24] carried out the experimental work on Inconel 600 on CNC wire EDM by L9 orthogonal array. The cryogenically tool wire was used for experimental work. As the current increases from 2 to 6 A and pulse on time from 50 to 100 μs it was observed that overcut was raised.

Prihandana et al. [25] investigated by application of shaker vibration to workpiece to make the hybrid EDM and the shaker does not pass vibration to tool. The surface roughness was best at 300 Hz in vibration assisted EDM at 0.75 μm amplitude. And for 1 μm amplitude Ra was good at 400 Hz. Goyal [26] performed ANOVA and SEM analysis on Inconel 625 wire EDM machining. Author designed the experiment with Taguchi in Minitab software and L18 orthogonal array was created. With increment in pulse on time from 105 to 125 μs the material elimination rate was improved from 4.7 to 7.4 mm^3/min at 10 A peak current. With cryogenic treated tool the MRR was better may be due to the abrasion. And within rise in peak current the Ra deteriorates due to larger surface layers erosion. Tsai et al. [27] research was based on vibration assisted EDM to make groove in titanium alloy with three different tool electrodes. The research findings demonstrate the material elimination rate was improved with vibration assisted setup which had voice coil motor in it. At 90 Hz the discharge time duration was two times less compared to unassisted EDM. Bhatt et al. [28] had conducted experiments on stainless steel with wire cut EDM. The experimental design was based on Taguchi and orthogonal array L27 was formulated using Minitab software. The optimum parameter found out using grey relational analysis were 112 μs pulse on time, 40 μs Toff, wire tension as 5 kgf, servo voltage being 24 V and optimized gap voltage was 50 V.

Shitara et al. [29] carried out their experimental research on panasonic micro EDM which had inbuilt RC pulse generator. The workpiece material was n-type 4H-SiC. It was concluded that the machining was greatly diminished with vibration assistance and at higher vibrational amplitude.

Kumawat et al. [30] machined the triangular profile on EN-31 steel utilizing wire EDM. The observations suggest that when current is heightened from 2 to 6A with Ton as 4 μs the material elimination rate improved from 25 to 29 mm^3/min. The optimized parameters determined were Ton & Toff as 4 μs, feed as 9 and current being 8A. Some investigations also carried out to enhance the characteristics of EDM variant process [35–37]. Also, researchers put efforts to modify the conventional EDM process with advance technology for various industrial applications [38–40]. In the present work comparative analysis of drilled hole with and without vibration assisted tool was performed. Machining was carried out on Inconel 625 which can be seen in Fig. 1 with copper tool. The composition of Inconel 625 is described below in Table 1.

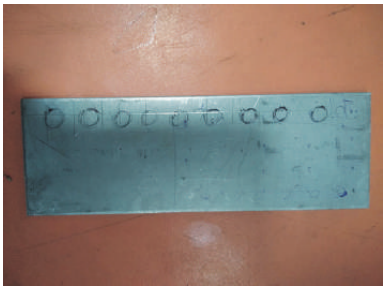

Fig. 1 Inconel 625 workpiece material used in experiments

2 Experiment details

The material vaporizing heat is generated in the EDM process by spark generated between tool and work material. Ionized dielectric fluid between tool and work carries electrons to bombard on the work material leaving it vaporized in the form of clouds. When clouds condensed and combined to form debris are taken away by the dielectric flow. Dielectric fluid plays very is important role in machining through EDM. Its effectiveness depends on dielectric constant which represents the electron holding capacity of the fluid and expressed as ratio of its electric permeability to the electric permeability of free space.

The present work, experiments has accomplished on ZNC-EDM machine tool (Savita Machine Tool Pvt Ltd Pune). Four parameters i.e., tool (normal and vibration assisted), peak current, pulse on time, pulse off time were varied to identify the effect on response parameters viz. surface roughness, cylindricity, and circularity. The workpiece thickness, tool diameter, and dielectric fluid were kept constant throughout the experiment. The Table 2 shows the design of experiment summary. The Inconel 625 (150 mm*50 mm*3 mm) is used to perform the experiments. It has a varied applications and enhances mechanical properties. The copper tool was used for this research work. Table 3 is a description of control factors used in the experiment and their different levels.

Table 1 Chemical composition of Inconel 625

Ni	Cr	Fe	Co	Mo	Nb	Ti	Al	C	Mn	Si
58	20–23	5	1	8–10	3.2–4.2	0.4	0.4	0.1	0.5	0.5

Table 2 Design of experiment summary

Taguchi array	L18(2^1 3^3)
Factors:	4
Runs:	18

First 9 experiments were made on normal die sink EDM which is shown in Fig. 2i based on the orthogonal array that was designed. Machining time was set to 2 min for each observation. For the remaining 9 experiments the vibration assisted tool system which is shown in Fig. 2ii. Coin vibration motor was affixed to cylindrical tool with the help of double-sided tape. Motor was soldered to zero PCB which was adhered to the tool. The power was supplied via 5 V battery. The specifications of motor are such that the outer diameter is 10 mm and thickness is 3 mm. The rated voltage is 1–6 V, current is 66 mA, output speed is 12000 rpm frequency 12 kHz.

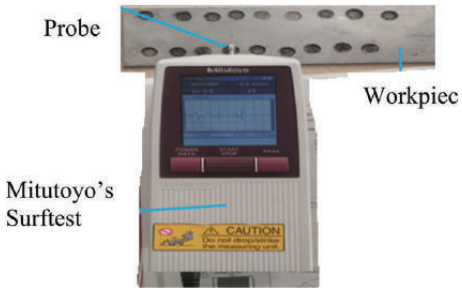

Fig. 3 Mitutoyo's SURFTEST (SJ-210)

Surface roughness of the machined surface was measured utilizing Mitutoyo's SURFTEST (SJ-210). Ra (roughness average) readings were noted with the same instrument. Figure 3 depicts the surface roughness tester utilized for the measurement. S/N ratio can be categorized into three domains, "smaller-is-better," "larger-is-better," and

Table 3 Control Factors and their levels

Symbol	Control factors	Units	Level 1	Level 2	Level 3
Tool	Tool electrode	–	Normal copper	Vibration assisted copper	–
Ip	Peak current	A	10	12	14
Ton	Pulse on time	µs	120	140	160
Toff	Pulse off time	µs	25	35	45

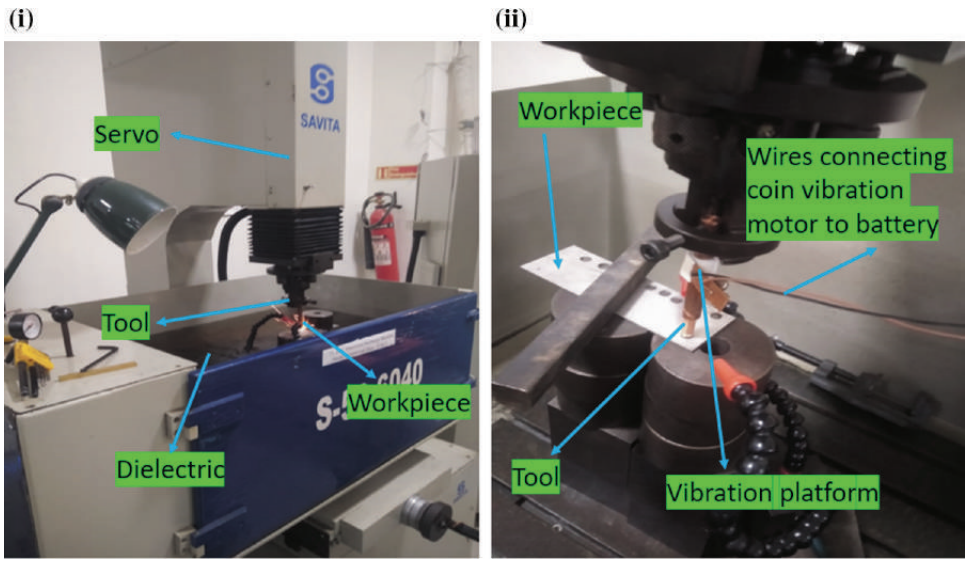

Fig. 2 (i) ZNC EDM Machine Tool, (ii) Vibration coin motor which is soldered to zero PCB is affixed to the tool with double side tape

"nominal-is-better." For surface roughness the S/N ratio utilized is smaller-is-better.

$$S/N = -10 * \log\left(\Sigma\left(Y_j\right)/n\right)) \tag{1}$$

where Y_j = numerical value of characteristic in jth observation and n = number of repetitions in a trial.

The circularity of the EDM drilled holes is using Mitutoyo Quick Image at RS India industry. S/N ratio for circularity is as follows.

$$S/N = -10 * \log\left(\Sigma\left(1/Y^2\right)/n\right) \tag{2}$$

2.1 Grey relational analysis (GRA)

It is utilized for finding the most optimal solution for give arrangements of parameters and which parameter to optimize. Initially there is a need to define the input variables and response variables [31]. The further step in GRA optimization is the normalization of response values on which optimization to be carried out. The microsoft excel should be utilized for doing calculations if there are large number of experiments on which GRA to be applied [32]. First make the column of response values [33]. Below the column make two rows of maximum and minimum values which can be inserted by using max and min formulae in the excel sheet. For smaller the better characteristics the normalized value is obtained by

$$X_i = \left(\frac{x_{\max} - x_i}{x_{\max} - x_{\min}}\right) \tag{3}$$

Next step is to calculate the deviation sequence. Subtract corresponding normalized value from 1 as it is the maximum value.

$$\Delta = (X_i)_{\max} - X_i \tag{4}$$

Further there is a need to calculate the grey relational coefficient. For that there is a requirement of delta max and min.

$$\zeta_i(k) = \frac{\Delta_{\min} + \zeta\,\Delta_{\max}}{\Delta_i + \zeta\,\Delta_{\max}} \tag{5}$$

The value of ζ is generally between 0 and 1. For the calculation purpose the value of ζ can be used as 0.5. Further step is to calculate the grey relational grade. This is calculated by average of grey relational coefficients.

$$\gamma_i = \frac{1}{n}\sum \zeta_i(k) \tag{6}$$

Based on grey relational grade these values are given rank. Larger value of grade means observed value are nearby ideal normalized values. Parameters corresponding to the highest rank are the optimum solution [34].

3 Result and discussion

The measured values of surface roughness along with calculated values of signal to noise ratios(db) employing "smaller is better" formula is obtained in Table 4. In the Fig. 4 there exist diagrams of main effect plots for SN ratios on surface roughness.

The experiment results demonstrate that better surface finish was obtained when utilizing copper tool without vibration which is shown in Fig. 4. It is possible that with the aid of vibration to the tool which was imparted by coin vibration motor setup the material is removed in large quantity and more layers are eroded. Due to this surface roughness may have increased. With the increment in the pulse on time first the surface roughness increases initially and then with further rise in Ton the surface roughness improves that is decreases. One possible reason can be that due to prolonged pulse on timing the crater depth increases which causes the surface roughness to increase. And further Toff also rises with Ton so that crater depth is less, and fine surface finish is seen.

When pulse off time is less, the time provided for flushing is less and debris are not eliminated properly so surface finish is poor. Peak current rise causes the surface roughness to increase because material is eliminated in bulk. In S/N ratio analysis, higher SN ration indicates significant value of the factor.

Interaction plot is read in a way such that straight graph lines convey a message that no interaction so far has been observed whereas any slope in the lines states that there is an interaction within various input factors. It is seen from Fig. 5 that for surface roughness as an output the interaction among tool, peak current, Ton and Toff is displayed.

Regression analysis is done to analyze how much each parameter is contributing to the output and what effect the input parameters have on output.

$$\begin{aligned} SR = {} & -1.323 + 0.5192\ \text{Tool} + 0.08658\ \text{Ip} \\ & + 0.000000\ \text{Ton} - 0.00001\ \text{Toff} \end{aligned} \tag{7}$$

With the help of signal to noise ratio graph that is displayed in Fig. 5 the optimum values of input parameters corresponding to peak in main effect plot for S/N ratio on surface roughness can be determined. This optimum combination is Tool1-Ip1-Ton2-Toff 2 which can be found from Table 5 where 1 and 2 being the levels.

Table 4 L18(2^1*3^3) orthogonal arrays and experimental results

S. No	Tool	Ip	Ton	Toff	SR (μm)	S/N
1	1	10	120	25	0.062	24.152
2	1	10	140	35	0.004	47.959
3	1	10	160	45	0.119	18.489
4	1	12	120	25	0.293	10.663
5	1	12	140	35	0.235	12.579
6	1	12	160	45	0.177	15.041
7	1	14	120	35	0.350	9.119
8	1	14	140	45	0.466	6.632
9	1	14	160	25	0.408	7.787
10	2	10	120	45	0.523	5.630
11	2	10	140	25	0.639	3.890
12	2	10	160	35	0.581	4.716
13	2	12	120	35	0.696	3.148
14	2	12	140	45	0.812	1.809
15	2	12	160	25	0.754	2.453
16	2	14	120	45	0.985	0.131
17	2	14	140	25	0.927	0.658
18	2	14	160	35	0.870	1.210

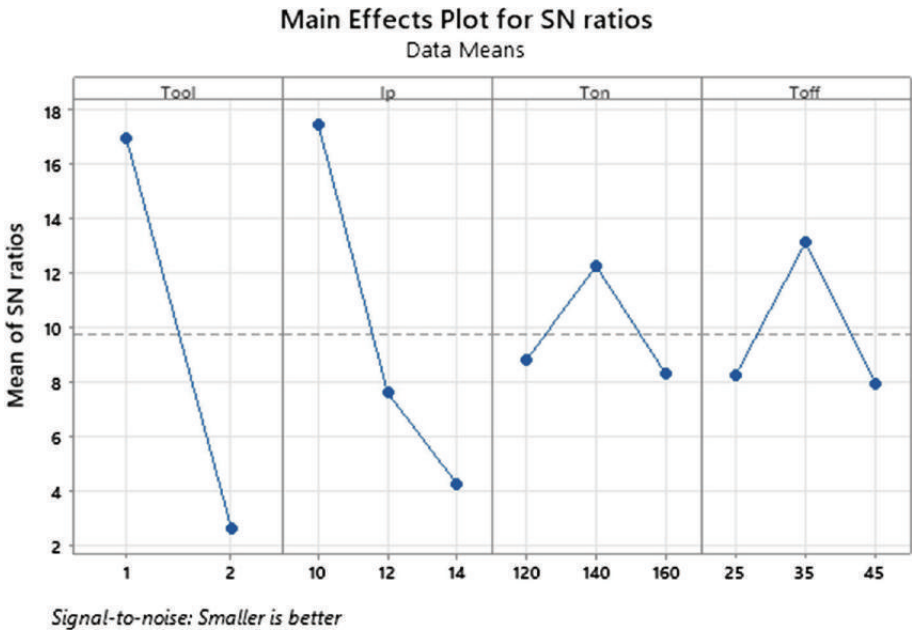

Fig. 4 Main effect plot for S/N ratio on surface roughness

Table 6 gives a detailed description of ANOVA table that is analysis of variance for the surface roughness. With this table the *P* values can be known for understanding the significant parameters in machining of Inconel 625 work material. In this table the input control factors whose *P* values are 0.05 or less than it is concluded as the statistically crucial for our present study of work. Hence it is evident that tool is the most significant parameter. And most significant parameter after tool is peak current. This also had very much crucial role in surface roughness obtained after machining the work material. And the remaining parameters does not have that much role to play in surface finish produced. The R-sq value comes out to be 97% from Table 7.

Residual plots are employed to check whether data is normal, does it possess non-random variation, does it have minimum variance etc. so basically it evaluates goodness-of-fit in analysis of variance and regression analysis. The Fig. 6 shows the residuals are almost normally distributed.

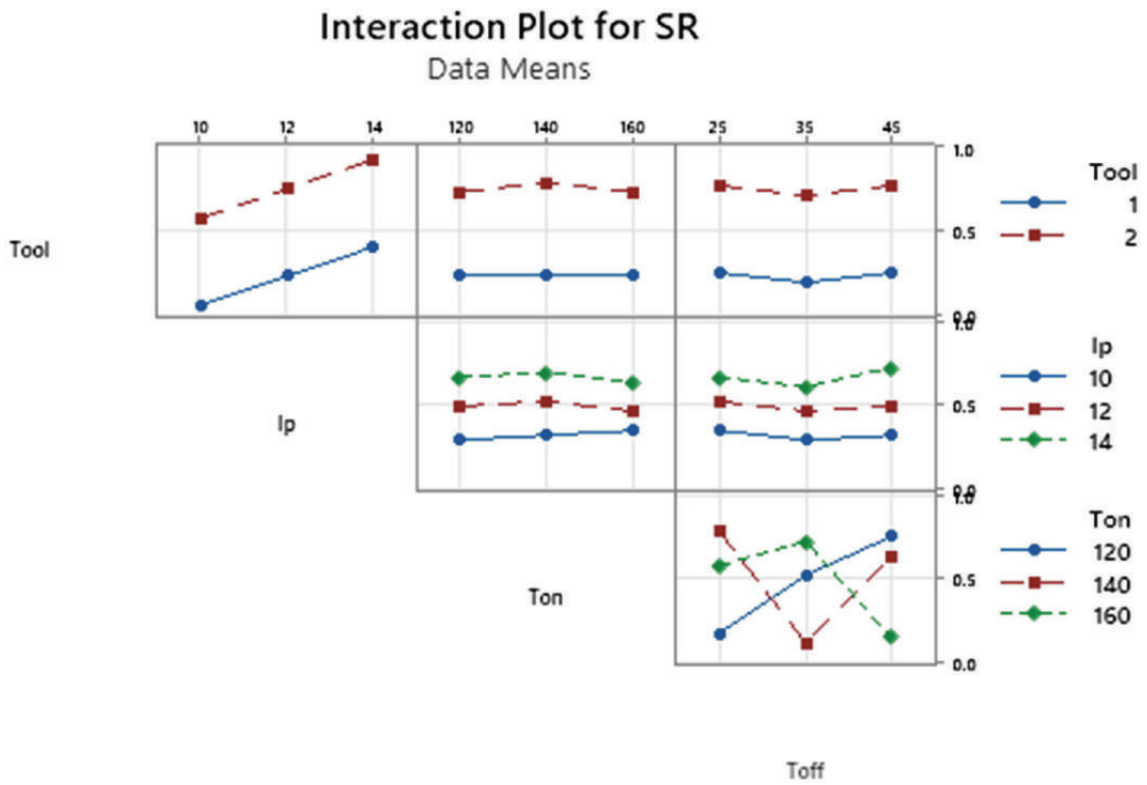

Fig. 5 Interaction plot for surface roughness

Table 5 Response table for S/N ratios (SR)

Level	Tool	Ip	Ton	Toff
1	16.936	17.473	8.807	8.267
2	2.627	7.615	12.254	13.122
3	–	4.256	8.283	7.955
Delta	14.308	13.217	3.972	5.166
Rank	1	2	4	3

Table 6 Analysis of Variance for SR

Source	DF	Adj SS	Adj MS	F-value	*P*-value
Regression	4	1.57300	0.39325	127.37	0.000
Tool	1	1.21316	1.21316	392.93	0.000
Ip	1	0.35984	0.35984	116.55	0.000
Ton	1	0.00000	0.00000	0.00	1.000
Toff	1	0.00000	0.00000	0.00	0.996
Error	13	0.04014	0.00309		
Total	17	1.61314			

Table 7 Model Summary SR

S	R-sq	R-sq(adj)	R-sq(pred)
0.0555652	97.51%	96.75%	95.14%

The Table 8 presents the measured results of the circular holes.

It is evident from Fig. 7 that circularity was better when no vibration was imparted to the tool, with the assistance of low frequency vibration the chances of ovality decreases. Because tool is vibrating due to eccentric rotating mass coin

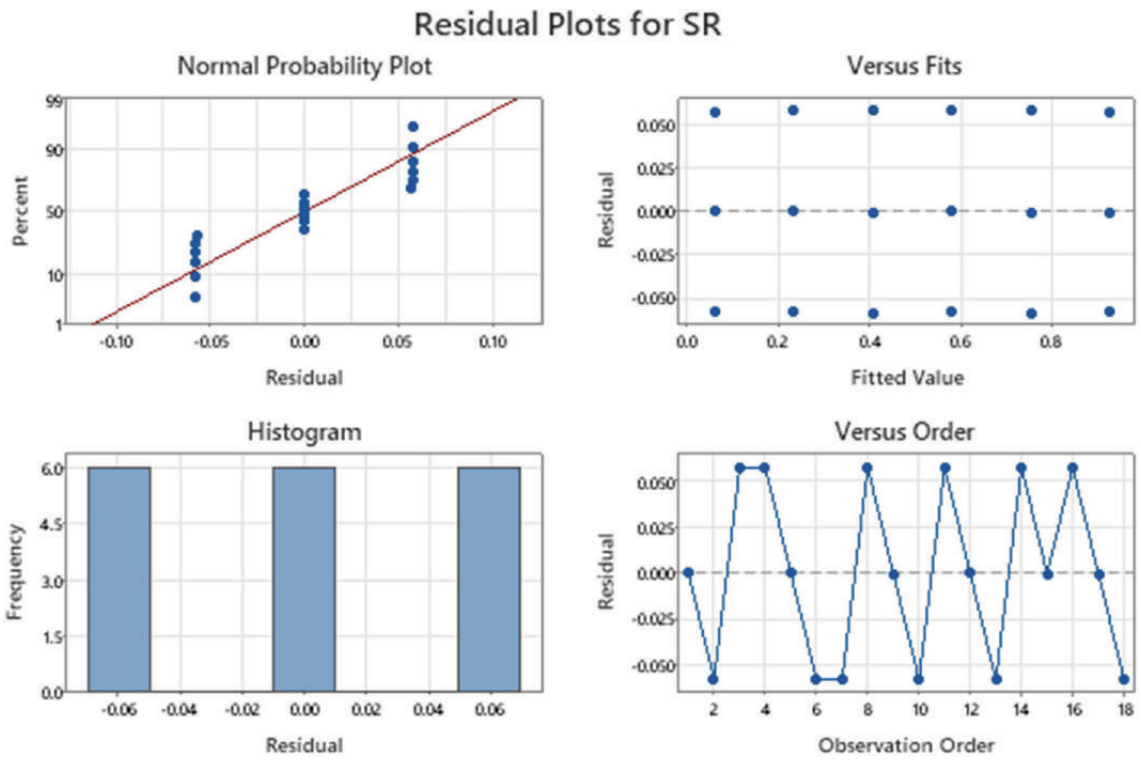

Fig. 6 Residual plots for surface roughness

Table 8 Results of circularity of holes

S. No	Tool	Ip	Ton	Toff	CIR	S/N
1	1	10	120	25	0.105	− 19.576
2	1	10	140	35	0.145	− 16.773
3	1	10	160	45	0.184	− 14.704
4	1	12	120	25	0.223	− 13.034
5	1	12	140	35	0.263	− 11.601
6	1	12	160	45	0.302	− 10.400
7	1	14	120	35	0.341	− 9.345
8	1	14	140	45	0.381	− 8.382
9	1	14	160	25	0.507	− 5.900
10	2	10	120	45	0.095	− 20.446
11	2	10	140	25	0.135	− 17.393
12	2	10	160	35	0.174	− 15.189
13	2	12	120	35	0.213	− 13.432
14	2	12	140	45	0.253	− 11.938
15	2	12	160	25	0.292	− 10.692
16	2	14	120	45	0.331	− 9.603
17	2	14	140	25	0.371	− 8.613
18	2	14	160	35	0.495	− 6.108

Fig. 7 Main effects plot for SN ratios on circularity

Table 9 Response Table for Signal to Noise Ratios on circularity

Level	Tool	Ip	Ton	Toff
1	− 12.190	− 17.347	− 14.239	− 12.535
2	− 12.602	− 11.849	− 12.450	− 12.075
3		− 7.992	− 10.499	− 12.579
Delta	0.411	9.355	3.741	0.504
Rank	4	1	2	3

shaped motor which causes uneven sparking and variable inter electrode gap. At peak current of 14 A and pulse on time of 160 μs the circularity is maximum as more material is eroded uniformly in circumferential direction as compared to 10 A.

With Table 9 it is clear that the optimum combination for circularity is Tool1-Ip3-Ton3-Toff2 where 1, 2 and 3 are the levels.

Also, in Fig. 8 is a description of interaction plot among input factors for the circularity. It is analyzed in a way that if there exist any parallel line it suggests no interaction and non-parallel line represent there is an interaction among parameters.

Regression equation

$$\begin{aligned} \text{CIR} = &-0.8629 - 0.0102\ \text{T} + 0.06617\ \text{Ip} \\ &+ 0.002692\ \text{Ton} - 0.000725\ \text{Toff} \end{aligned} \tag{8}$$

It can be concluded that every parameter has some contribution in circularity calculation unlike surface roughness which was independent of pulse on time.

Table 10 gives analysis of variance of circularity output parameter. It has been observed from ANOVA table that peak current and Ton are the significant parameters as their p value is less than 0.05. The R-sq value comes out to be 97% from Table 11.

Figure 9 is the graphical representation of residual plots of circularity. It can be described that straight line is there in normal probability plot. Residuals are randomly distributed on either side of base line. Hence residuals are interdependent.

Table 12 gives a detailed description of GRA optimization applied on surface roughness and circularity response values. First data has been normalized in MS Excel. Further, deviation sequence and grey relational coefficient has been determined. Now critical step is grey relational grade which is the average of all the grey relational coefficient corresponding to given outputs. In the end rank has been determined.

The row 9 seems to be getting rank as one. Hence outputs corresponding to the row 9 are the optimum which are surface roughness as 0.408 μm and circularity as 0.507. And the optimum input values corresponding to these outputs are Tool be 1, Ip as 14 A, Ton is 160 μs and Toff is 25 μs.

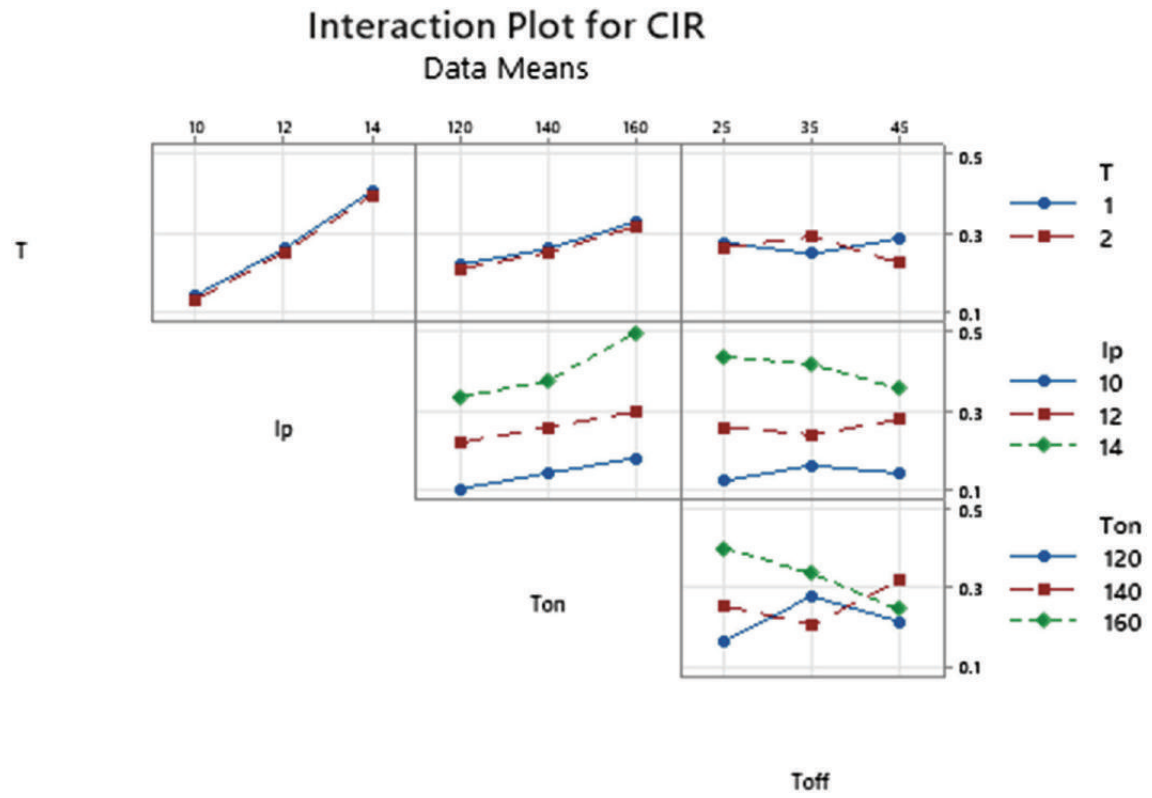

Fig. 8 Interaction plot for circularity

Table 10 Analysis of variance for CIR

Source	DF	Adj SS	Adj MS	F-value	*P*-value
Regression	4	0.246023	0.061506	106.15	0.000
T	1	0.000470	0.000470	0.81	0.384
Ip	1	0.210145	0.210145	362.68	0.000
Ton	1	0.034776	0.034776	60.02	0.000
Toff	1	0.000631	0.000631	1.09	0.316
Error	13	0.007532	0.000579		
Total	17	0.253555			

Table 11 Model summary CIR

S	R-sq (%)	R-sq(adj) (%)	R-sq(pred) (%)
0.0240712	97.03	96.12	93.80

3.1 Microstructure analysis

The drilled hole on EDM machine tool was observed using Field Emission Scanning Electron Microscope. Four samples were investigated two machined with normal copper tool and two using vibration assisted Cu tool.

3.2 SEM analysis

After machining operation on Inconel 625 workpiece the four samples of size 1 by 1 cm were cut from machined sample out of 18-hole samples. These samples were cut using wire EDM. It is observed the Inconel 625 job undergoes structure

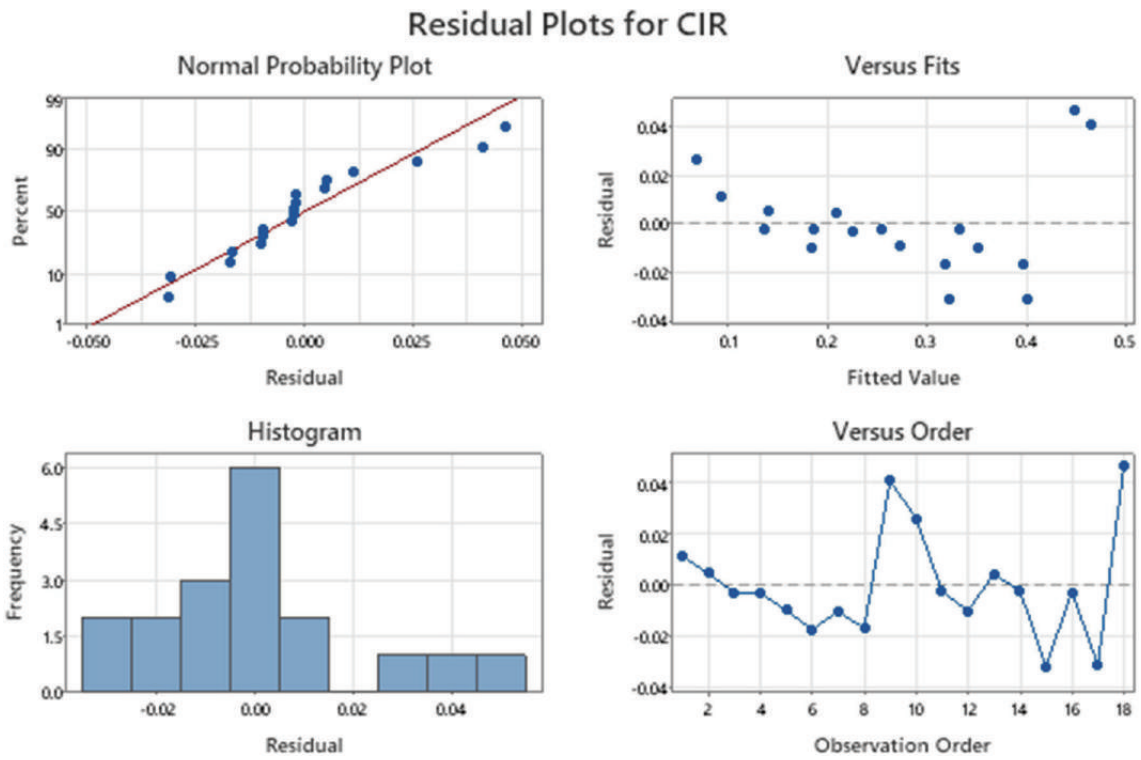

Fig. 9 Residual plots for circularity

Table 12 Multi objective optimization using grey relational analysis

S No	SR	CIR	Normalized values		Deviation sequence		Grey relational coefficient		GRG	Rank
			SR	CIR	SR	CIR	SR	CIR		
1	0.062	0.105	0.941	0.024	0.059	0.976	0.894	0.339	0.617	5
2	0.004	0.145	1.000	0.121	0.000	0.879	1.000	0.363	0.681	2
3	0.119	0.184	0.883	0.216	0.117	0.784	0.810	0.389	0.600	6
4	0.293	0.223	0.705	0.311	0.295	0.689	0.629	0.420	0.525	10
5	0.235	0.263	0.765	0.408	0.235	0.592	0.680	0.458	0.569	8
6	0.177	0.302	0.824	0.502	0.176	0.498	0.739	0.501	0.620	4
7	0.35	0.341	0.647	0.597	0.353	0.403	0.586	0.554	0.570	7
8	0.466	0.381	0.529	0.694	0.471	0.306	0.515	0.620	0.568	9
9	0.408	0.507	0.588	1.000	0.412	0.000	0.548	1.000	0.774	1
10	0.523	0.095	0.471	0.000	0.529	1.000	0.486	0.333	0.410	17
11	0.639	0.135	0.353	0.097	0.647	0.903	0.436	0.356	0.396	18
12	0.581	0.174	0.412	0.192	0.588	0.808	0.459	0.382	0.421	14
13	0.696	0.213	0.295	0.286	0.705	0.714	0.415	0.412	0.413	15
14	0.812	0.253	0.176	0.383	0.824	0.617	0.378	0.448	0.413	16
15	0.754	0.292	0.235	0.478	0.765	0.522	0.395	0.489	0.442	12
16	0.985	0.331	0.000	0.573	1.000	0.427	0.333	0.539	0.436	13
17	0.927	0.371	0.059	0.670	0.941	0.330	0.347	0.602	0.475	11
18	0.87	0.495	0.117	0.971	0.883	0.029	0.362	0.945	0.653	3

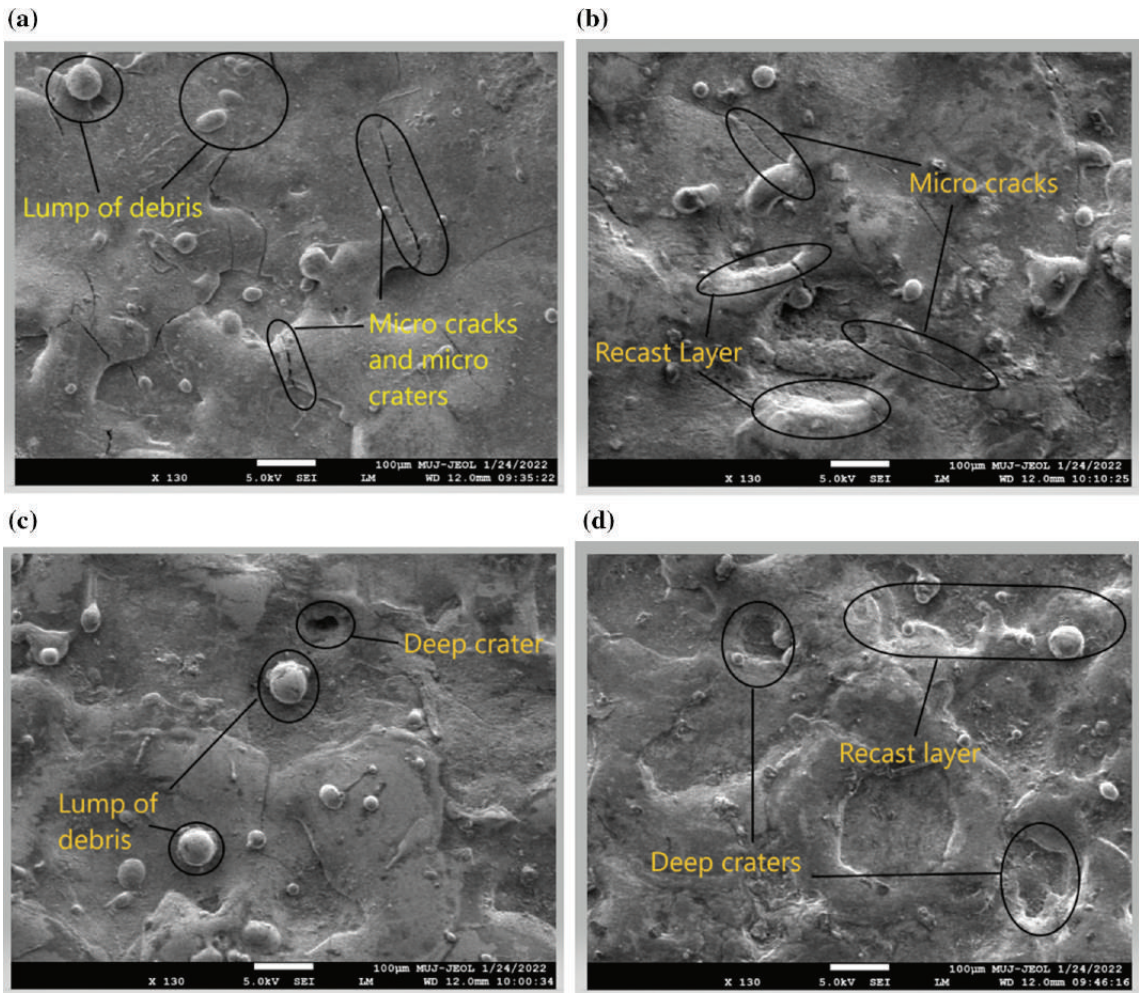

Fig. 10 **a** SEM image of Exp no 1 **b** SEM image of Exp no 9 **c** SEM image of Exp no 10 **d** SEM image of Exp no 15

wise change on micro level. Figure 10a states SEM image of experiment no 1 that is Tool 1, Ip 10 A, Ton 120 μs and Toff 25 μs at 100 μm with X 130. Here micro cracks and micro craters are present.

Figure 10b represents the SEM image of experiment no 9 where Tool 1, Ip 14A, Ton 160 μs and Toff 25 μs have been used. In both experiment 1 and 9 which is shown in Fig. 10a and Fig. 10b respectively no vibration was present during machining. In the Fig. 10b the droplets are clearly visible due to high current and large pulse on time. It is called as recast layer that is metal once removed in form of debris during evaporation is settled back as cloud solidifies.

Figure 10c is the SEM photo of experiment no 10 having Tool 2, Ip 10A, Ton 120 μs and Toff 45 μs. The lump of debris and recast layer is visible in the SEM image. One deep crater is also visible in this image. In this case vibration assisted tool was used. This decreased the surface roughness of machined surface relatively. Figure 10d is the SEM photo of experiment no 15 having Tool 2, Ip 12A, Ton 160 μs and Toff 25 μs. Deep craters are visible due to high pulse on time. Due to presence of vibration on tool it is seen the recast layer is formed.

3.3 EDS analysis

For the Exp 1 and Exp 9 the percentage of Cu deposition was found to be 1.4% and 1.8% respectively. In Exp 9 percentage of Cu, which is shown in Figs. 11a and 12, is higher because due to high current recast layer is developed after condensation of vaporized cloud of debris. Hence it has been verified that machining was done with copper tool.

For the exp 10 and exp 15 the percentage of Cu deposition was found to be 1% and 1.4%. The percentage of Cu is found to be less when machining was done with the help of vibration assisted tool. It is because the vibration of tool generates flushing effect due to which less amount of tool wear particles is deposited.

(a)

Element	Weight %	Atomic %	Error %
C K	16.1	42.4	12.2
O K	8.1	16	12.4
NiL	34.6	18.7	8.4
AlK	0.7	0.8	30.9
SiK	0.7	0.8	23.9
NbL	2.8	1	14.1
MoL	6.7	2.2	10.5
TiK	0.7	0.5	24.5
CrK	22.5	13.7	3.5
MnK	1.1	0.6	32.3
FeK	4.1	2.3	10.7
CuK	1.8	0.9	24.5

(b)

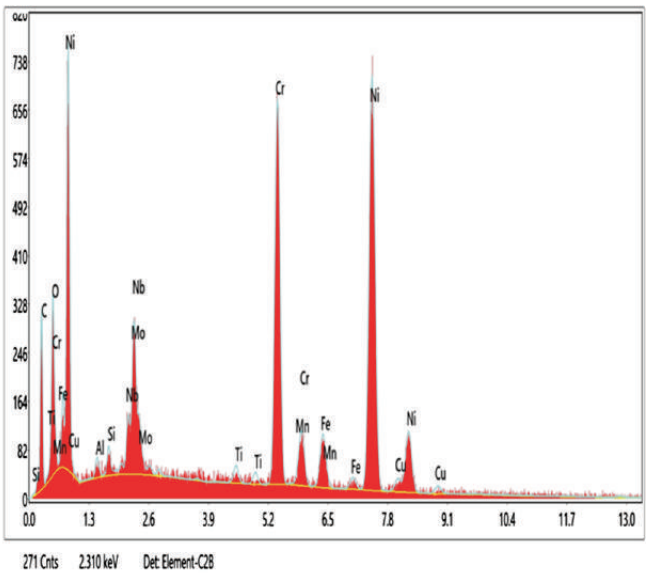

Fig. 11 **a** Chemical Composition of elements present after machining in exp. no. 9, **b** EDS analysis of sample generated in exp. No. 9 with kV: 20 and Resolution:(eV) 130

(a)

Element	Weight %	Atomic %	Error %
C K	11.5	33.7	12.3
O K	8	17.5	11.2
SiK	0.5	0.7	21.6
NbL	2.1	0.8	13.7
MoL	4.4	1.6	11.7
TiK	0.6	0.4	26.4
CrK	19.8	13.4	3.3
MnK	1.1	0.7	24.3
FeK	4.5	2.8	8.7
NiK	46.5	27.8	3
CuK	1	0.6	43.3

(b)

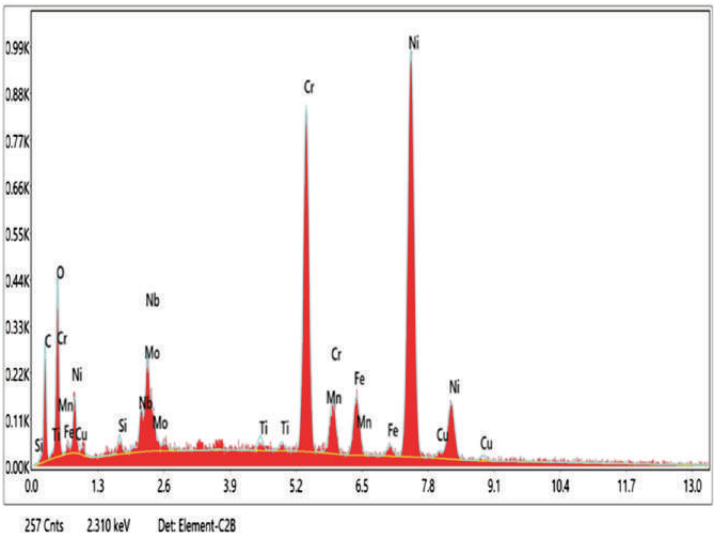

Fig. 12 **a** Chemical composition of elements after vibration assisted machining in exp. no. 10, **b** EDS analysis of sample generated in exp. no. 10

4 Conclusion

The experiments have been performed by using the vibration set up and normal Micro-EDM machining. After obtaining the optimize result and material characterization results the following conclusions has been made.

1. Surface roughness of machining specimen significantly depends on nature of tool and peak current.
2. Pulse on time and peak current are the significant factors affecting the circularity of the drilled hole.
3. Surface finish was good when no vibration was present on tool.
4. Circularity improves by 145% when Toff was raised from 35 to 45 μs. But, with the vibration the circularity of hole decreases.
5. GRA optimization technique used to find optimum values of surface roughness, as 0.408 μm and circularity as 0.507 linked with experiment number 9 of L18. Optimum input values corresponding to these outputs are Tool be 1, Ip as 14 A, Ton is 160 μs and Toff is 25 μs. Combination of these input value will deliver the minimum surface roughness and maximum circularity.
6. In microstructure analysis it is found that less recast deposition is found in vibration assisted EDM.
7. EDS analysis reveals that copper percentage is less with vibration assisted EDM indicating effective flushing of debris.

References

1. Talla, G., Gangopadhyay, S., Biswas, C.K.: Effect of powder-suspended dielectric on the EDM characteristics of Inconel 625. J. Mater. Eng. Perform. **25**(2), 704–717 (2015). https://doi.org/10.1007/S11665-015-1835-0
2. Subrahmanyam, M., Nancharaiah, T.: Optimization of process parameters in wire-cut EDM of Inconel 625 using Taguchi's approach. Mater. Today: Proc. **23**, 642–646 (2020). https://doi.org/10.1016/j.matpr.2019.05.449
3. Mausam, K., Kumar Singh, P., Sharma, K., Gupta, R.C.: Investigation of process parameter of EDM using genetic algorithm (GA) approach for carbon fiber based two phase epoxy composites. Mater. Today: Proc. **3**(10), 4102–4108 (2016). https://doi.org/10.1016/j.matpr.2016.11.081
4. Mertiya, A.S., et al.: Development and investigation of an inexpensive low frequency vibration platform for enhancing the performance of electrical discharge machining process. Materials **14**(20), 6192 (2021). https://doi.org/10.3390/ma14206192
5. Teimouri, R., Baseri, H.: Improvement of dry EDM process characteristics using artificial soft computing methodologies. Prod. Eng. Res. Dev. **6**(4–5), 493–504 (2012). https://doi.org/10.1007/s11740-012-0398-2
6. Goyal, A., Pandey, A., Sharma, P.: Machinability of Inconel 625 aerospace material using cryogenically treated WEDM. Solid State Phenom. **266**, 38–42 (2017). https://doi.org/10.4028/WWW.SCIENTIFIC.NET/SSP.266.38
7. Goyal, A., Pandey, A., Sharma, P.: Investigation of surface roughness for Inconel 625 using wire electric discharge machining. IOP Conf. Ser. Mater. Sci. Eng. **377**(1), 012109 (2018). https://doi.org/10.1088/1757-899X/377/1/012109
8. Unune, D.R., Nirala, C.K., Mali, H.S.: Accuracy and quality of micro-holes in vibration assisted micro-electro-discharge drilling of Inconel 718. Measurement **135**, 424–437 (2019). https://doi.org/10.1016/J.MEASUREMENT.2018.11.067
9. Teimouri, R., Baseri, H.: Experimental study of rotary magnetic field-assisted dry EDM with ultrasonic vibration of workpiece. Int. J. Adv. Manuf. Technol. **67**(5), 1371–1384 (2012). https://doi.org/10.1007/S00170-012-4573-6
10. Somashekhar, K.P., Ramachandran, N., Mathew, J.: Optimization of material removal rate in micro-EDM using artificial neural network and genetic algorithms. Mater. Manuf. Process. **25**(6), 467–475 (2010). https://doi.org/10.1080/10426910903365760
11. Srivastava, V., Pandey, P.M.: Effect of process parameters on the performance of EDM process with ultrasonic assisted cryogenically cooled electrode. J. Manuf. Process. **14**(3), 393–402 (2012). https://doi.org/10.1016/J.JMAPRO.2012.05.001
12. Zhang, L., Jia, Z., Wang, F., Liu, W.: A hybrid model using supporting vector machine and multi-objective genetic algorithm for processing parameters optimization in micro-EDM. Int. J. Adv. Manuf. Technol. **51**(5–8), 575–586 (2010). https://doi.org/10.1007/s00170-010-2623-5
13. Unune, D.R., Mali, H.S.: Experimental investigation on low-frequency vibration-assisted μ-ED milling of Inconel 718. Eng. Sci. Technol. Int. J. **20**(1), 222–231 (2017). https://doi.org/10.1016/j.jestch.2016.06.010
14. Kumar, A., Kumar, V., Kumar, J.: Surface crack density and recast layer thickness analysis in WEDM process through response surface methodology. Mach. Sci. Technol. **20**(2), 201–230 (2016). https://doi.org/10.1080/10910344.2016.1165835
15. Huu, P.N., et al.: Multi-objective optimization of process parameter in EDM using low-frequency vibration of workpiece assigned for SKD61. Sadhana Acad. Proc. Eng. Sci. (2019). https://doi.org/10.1007/S12046-019-1185-Y
16. Mohanty, C.P., Mahapatra, S.S., Singh, M.R.: An intelligent approach to optimize the EDM process parameters using utility concept and QPSO algorithm. Eng. Sci. Technol. Int. J. **20**(2), 552–562 (2017). https://doi.org/10.1016/j.jestch.2016.07.003
17. Endo, T., Tsujimoto, T., Mitsui, K.: Study of vibration-assisted micro-EDM—the effect of vibration on machining time and stability of discharge. Precis. Eng. **32**(4), 269–277 (2008). https://doi.org/10.1016/J.PRECISIONENG.2007.09.003
18. Rahul, S., Datta, B., Biswal, B., Mahapatra, S.S.: A novel satisfaction function and distance-based approach for machining performance optimization during electro-discharge machining on super alloy inconel 718. Arab. J. Sci. Eng. **42**(5), 1999–2020 (2017). https://doi.org/10.1007/s13369-017-2422-5
19. Lee, P.A., Kim, Y., Kim, B.H.: Effect of low frequency vibration on micro EDM drilling. Int. J. Precis. Eng. Manuf. **16**(13), 2617–2622 (2015). https://doi.org/10.1007/S12541-015-0335-3
20. Kumar, S., Gupta, A.K., Chandna, P., Bhushan, G., Kumar, A.: A novel approach of GEF and GA for the optimization of multi-objective wire EDM process during the machining of DC53 super alloy. Proc. Inst. Mech. Eng. Part E J. Process Mech. Eng. **235**(4), 1119–1131 (2021). https://doi.org/10.1177/0954408921992918
21. Le, Q.D., Nguyen, H.P., Banh, T.L., Nguyen, D.T.: Comparative study of low-frequency vibrations assigned to a workpiece in EDM and PMEDM. Int. J. Mod. Phys. B (2020). https://doi.org/10.1142/S0217979220401451
22. Kumaran, S.T., Ko, T.J., Kurniawan, R.: Grey fuzzy optimization of ultrasonic-assisted EDM process parameters for deburring CFRP composites. Meas. J. Int. Meas. Confed. **123**, 203–212 (2018). https://doi.org/10.1016/j.measurement.2018.03.076

23. Nguyen, H.P., Ngo, N.V., Nguyen, Q.T.: Optimizing process parameters in edm using low frequency vibration for material removal rate and surface roughness. J. King Saud Univ. Eng. Sci, **33**(4), 284–291 (2021). https://doi.org/10.1016/j.jksues.2020.05.002
24. Pandey, A., Goyal, A., Meghvanshi, R.: Experimental Investigation and optimization of machining parameters of aerospace material using taguchi's DOE approach. Mater. Today Proc. **4**(8), 7246–7251 (2017). https://doi.org/10.1016/J.MATPR.2017.07.053
25. Prihandana, G.S., Mahardika, M., Hamdi, M., Mitsui, K.: Effect of low-frequency vibration on workpiece in EDM processes. J. Mech. Sci. Technol. **25**(5), 1231–1234 (2011). https://doi.org/10.1007/S12206-011-0307-1
26. Goyal, A.: Investigation of material removal rate and surface roughness during wire electrical discharge machining (WEDM) of Inconel 625 super alloy by cryogenic treated tool electrode. J. King Saud Univ. Sci. **29**(4), 528–535 (2017). https://doi.org/10.1016/J.JKSUS.2017.06.005
27. Tsai, M.Y., Fang, C.S., Yen, M.H.: Vibration-assisted electrical discharge machining of grooves in a titanium alloy (Ti-6A-4V). Int, J. Adv. Manuf. Technol. **97**(1), 297–304 (2018). https://doi.org/10.1007/S00170-018-1904-2
28. Bhatt, D., Goyal, A.: Multi-objective optimization of machining parameters in wire EDM for AISI-304. Mater. Today Proc. **18**, 4227–4242 (2019). https://doi.org/10.1016/J.MATPR.2019.07.381
29. Shitara, T., Fujita, K., Yan, J.: Direct observation of discharging phenomena in vibration-assisted micro-electrical discharge machining. Int. J. Adv. Manuf. Technol. **108**(4), 1125–1138 (2020). https://doi.org/10.1007/S00170-019-04877-7
30. Kumawat, A., Goyal, A., Dadhich, M., Gupta, R.: Development and optimization of triangular profile by using wire EDM machining process. Mater. Today Proc. **28**, 2369–2374 (2020). https://doi.org/10.1016/J.MATPR.2020.04.645
31. Muthu, P.: Multi objective optimization of wear behaviour of aluminum MMCs using Grey-Taguchi method. Manuf. Rev. (2020). https://doi.org/10.1051/mfreview/2020013
32. Jung, J.H., Kwon, W.T.: Optimization of EDM process for multiple performance characteristics using Taguchi method and Grey relational analysis. J. Mech. Sci. Technol. **24**,1083–1090 (2010). https://doi.org/10.1007/s12206-010-0305-8
33. Singh, O., Kumar, G., Electronica, M.K.A, et al.: Role of taguchi and grey relational method in optimization of machining parameters of different materials: a review. Acta. Electron. Malays. **3**(1), 19–22 (2019). https://doi.org/10.26480/aem.01.2019.19.22
34. Lin, Y.C., Lee, H.S.: Optimization of machining parameters using magnetic-force-assisted EDM based on gray relational analysis. Int. J. Adv. Manuf. Technol. **42**(11–12), 1052–1064 (2009). https://doi.org/10.1007/S00170-008-1662-7
35. Palanisamy, D., Manikandan, N., Ramesh, R., Kathirvelan, M., Arulkirubakaran, D.: Machinability analysis and optimization of wire-EDM textured conventional tungsten carbide inserts in machining of 17–4 PH stainless steel. Mater. Today Proc. **1**(39), 359–367 (2021)
36. Manikandan, N., Arulkirubakaran, D., Palanisamy, D., Raju, R.: Influence of wire-EDM textured conventional tungsten carbide inserts in machining of aerospace materials (Ti–6Al–4V alloy). Mater. Manuf. Process. **34**(1), 103–111 (2019)
37. Arunbharathi, R., Varthanan, P.A., Akilesh, M., Raju, R.A., Kumar, G.A.: Experimental investigation and optimization of process parameters in WEDM on machining of H13 steel using response surface methodology. Indian J. Eng. Sci. Technol. **11**(1), 39 (2017)
38. Kale, B.S., Bhole, K.S., Dhongadi, H., Oak, S., Deshmukh, P., Oza, A., Ramesh, R.: Effect of polygonal surfaces on development of viscous fingering in lifting plate Hele-Shaw cell. Int. J. Interact. Des. Manuf. IJIDeM (2022). https://doi.org/10.1007/s12008-022-01030-9
39. Shinde, S.M., Lekurwale, R.R., Bhole, K.S., Oza, A.D., Patil, A.S., Ramesh, R.: 5-axis virtual machine tool centre building in PLM environment. Int. J. Interact. Des. Manuf. IJIDeM (2022). https://doi.org/10.1007/s12008-022-00974-2
40. Gautam, N., Goyal, A., Sharma, S.S., Oza, A.D., Kumar, R.: Study of various optimization techniques for electric discharge machining and electrochemical machining processes. Mater. Today: Proc. **57**, 615–621 (2022)